Journal of the Serbian Chemical Society
JSCS-info@shd.org.rs • www.shd.org.rs/JSCS

ACCEPTED MANUSCRIPT

Journal of the Serbian Chemical Society
JSCS-info@shd.org.rs • www.shd.org.rs/JSCS
*J. Serb. Chem. Soc.***00(0)** 1-16 (2024)
JSCS–12826
Original scientific paper
Published DD MM, 2024

Enhanced adsorption properties of Algerian bentonite modified by starch and glycerol for methylene blue and red methyl retention

FATIMA ZAHRA BENHACHEM[1,2]*, HANANE MAHROUG[2,3], MERIEM BENDJELLOUL[4], ABDELKADER MIRAOUI[1,2], EL HADJ ELANDALOUSSI[4], KHALIL OUKEBDANE[2], RANIA HALFAOUI[5]

[1]Department of Industrial Engineering, Faculty of Technology, University of Tlemcen, Tlemcen, Algeria, [2]Laboratory of Separation and Purification Technologies, Department of Chemistry, Faculty of Sciences, University of Tlemcen, Tlemcen, Algeria, [3]Department of Hydraulic, Institute of Sciences and Technology, University center of Maghnia, Algeria. [4]Environment and Sustainable Development Laboratory, Department of Chemistry, Faculty of Sciences and Technology, University of Relizane, Algeria, and [5]Department of Chemistry, Faculty of Sciences, University of Tlemcen, Tlemcen, Algeria.

(Received 29 February; revised 22 April; accepted 24 November 2024)

Abstract: This paper describes the preparation of novel bentonite-starch composites, and assesses their effectiveness as adsorbents for removing methylene blue (MB) and methyl red (MR) dyes from aqueous solutions. The adsorbents were characterized using X-ray diffraction and FTIR spectroscopy. The study aimed to optimize the removal process by investigating the effect of pH, adsorbent dose, contact time, and initial concentration. The sorption kinetics of MB and MR dyes were analyzed using the pseudo-first order and pseudo-second-order models. The experimental results indicate that the pseudo-second order kinetic model provides the best fit. The composite adsorbents exhibited a sorption capacity for MB, ranging from 146.21 mg g^{-1} to 157.58 mg g^{-1} for bentonite-starch (Bt@star) and bentonite-starch-glycerol (Bt@star@gly), respectively. The sorption capacity for MR dye was 426.38 mg g^{-1} for Bt@star and 309.82 mg g^{-1} for Bt@star@gly. Furthermore, the correlation coefficient values indicate that the adsorption of MB and MR by Bt@star@gly is best described by the Langmuir model. This unequivocally implies that the adsorbent surface is homogeneous, resulting in monolayer adsorption. The Langmuir model also accurately describes the adsorption of MB onto Bt@Star. However, the Freundlich isotherm model is the best fit for the adsorption of MR, indicating the existence of multilayer adsorption. Finally, this study demonstrates that the composite adsorbents prepared herewith exhibit excellent adsorption performance and can be a cost-effective alternative for treating colored wastewater.

* Corresponding author. E-mail: f.benhachem@yahoo.com
https://doi.org/10.2298/JSC240219108B

Keywords: composite; dyes; wastewater; kinetics.

INTRODUCTION

Organic dyes are synthetic compounds extensively used in industries like textiles, paper, and plastics.[1] However, their stability and resistance to degradation make them persistent environmental pollutants.[2] When discharged into water bodies, these dyes can cause severe water pollution, affecting aquatic life and potentially entering the human food chain.[3] Effective removal of organic dyes from wastewater is crucial to prevent environmental contamination and safeguard public health.[4]

Recently, various methods and technologies have been proposed and utilized for treating wastewater contaminated with dyes. These methods include membrane filtration,[5] biological treatment,[6] oxidation, photocatalytic degradation,[7] adsorption[8] and coagulation-flocculation.[9] Researchers widely use the adsorption method as an alternative for dye wastewater treatment.[10] However, the efficiency of this process can be limited by the use of expensive adsorbents.[11]

One of the most effective techniques for improving the adsorption process is to use various mineral or cement additives. These additives can be of natural origin, such as natural pozzolan, or artificial, such as lime or cement. They can also be mineral waste, such as silica fume, fly ash and so on. These materials exhibit distinct physicochemical and mineralogical characteristics. [12] Furthermore, low-cost materials, such as natural adsorbents, agricultural waste, and by-products, have been proven effective in removing dyes.[13] Clay minerals are considered as alternative materials to achieve this goal. According to many studies, bentonite clay can improve their properties in several fields.[14] Bentonites are clay minerals, formed mainly by smectitic minerals in the form of lamellar silicates. In these minerals, their small particle size, less than 4 μm,[15] creates a large specific surface area, and the presence of charge on the surfaces gives them unique physicochemical properties that allow them to attract substances from aqueous solutions. They are therefore widely used, among other important applications, to adsorb toxic compounds from aqueous media.[16]

However, it is a simple fact that clays have a low affinity for negatively charged anionic dyes. It is important to note that the adsorption capacities of clays can be significantly enhanced through a simple modification process using cationic polymers or surfactants. This can be achieved through straightforward ion-exchange reactions that create interactions between the cationic species and the adsorbate.[17] Previous research has shown that using modified montmorillonite instead of raw montmorillonite greatly increases the effectiveness of acid dye removal.[18] It is important to note that he synthesis of modified montmorillonites has already been reported and successfully used for the adsorption of Congo Red dye.[19] The study showed that the adsorption efficiency was significantly affected

by the length of alkyl chains in a series of alkyl ammonium bromides. Several authors have successfully modified montmorillonite using unconventional agents,[20] including gemini surfactants, to improve the adsorption of organic contaminants.[21]

This paper outlines a new approach for the modification of bentonite with starch and glycerol. The prepared composites were used as adsorbents to remove cationic (Methylene Blue) and anionic (Methyl Red) dyes. Various experimental parameters were examined to optimize the adsorption conditions. To assess the adsorption process, some kinetic studies were carried out.

EXPERIMENTAL

Materials

The material used in this study is the natural clay of Maghnia (Algeria), which is supplied by the ENOF company of bentonites.

One portion of the clay was used in the experiments, while the other was utilized for composite preparation. The procedure given for the preparation of the Bt@star@gly composite consists of mixing 5 g (5%) bentonite in 45 mL of distilled water, and then adding 0.75 g (30%) glycerol and 0.125 g (5%) starch to the suspension. On the other hand, the second composite (Bt@star) was prepared by the mixing of equal amounts by weight of bentonite and starch. The mixtures were then refluxed at a temperature of 80 °C for 4 hours. After evaporating the water under reduced pressure, the resulting composites were manually ground and purified by stirring for 2 hours in distilled water to remove unreacted starting materials. Finally, the purified bio-composites were dried in an electric oven at 60°C for 24 h.

The synthesized composites were evaluated for their mineralogical and structural properties using X-ray diffraction (XRD) with Copper Kα radiation (λ = 1.54 Å) at 40 kV and 30 mA, on a Rigaku Mini Flex 600. Fourier-transform infrared spectroscopy (FTIR) studies were conducted using the Agilent Cary 600 Series FTIR. Transmission spectra were obtained in the range of 4000–400 cm^{-1}.

Adsorption experiments

Batch equilibrium experiments were conducted to evaluate the adsorption capacities of the prepared composites for Methylene Blue (MB) and Methyl Red (MR). In each experiment, 25 mg of the composites were added to 25 ml of dye solutions with initial dye concentrations of 100 mg/L^{-1}. The experiments were carried out in beakers with constant stirring at 400 rpm. The pH of the solution was adjusted within the range of 3 to 9 by the addition of drops of 1 M HCl or NaOH solutions. The contact time ranged from 5 to 120 minutes, while the initial dye concentration ranged from 100 to 500 mg/L^{-1}. After adsorption, the adsorbent was separated from the liquid phase by centrifugation at 3000 rpm for 10 minutes. The supernatant was analyzed using an OPTIZEN 1412 UV/VIS spectrophotometer.

The adsorption capacity and removal efficiency were calculated from the initial and final concentrations of the dyes in the solution using the following equations:

$$q_e = (C_o - C_e)\, V/m \quad (1)$$

$$RE\ (\%) = 100\ (C_o - C_e)/\ C_o \quad (2)$$

where C_o and C_e denote the initial and equilibrium concentrations (mg/L^{-1}) of the dye aqueous solution, V represents the volume of the dye solution (L), and m represents the mass (g) of the adsorbent used in each experiment.

RESULTS AND DISCUSSION

Adsorbents characterizations

Raw bentonite Bt, Bt@star, and Bt@star@gly adsorbent materials were characterized using XRD and FTIR techniques. The XRD diffractogram of raw bentonite, shown in Figure 1a, indicates the presence of different diffraction peaks at 5.84°, 15.71°, 19.96°, 21°, 26.8°, 35.1°, 42.62°, 46.02°, 50.28°, 54.82°, 62.15°, 68.32°, and 73.28°, corresponding to different phases such as montmorillonite, quartz, calcite, and magnesite.

These peaks were also observed in the biocomposites Bt@star and Bt@star@gly, with a single characteristic peak at 2θ = 5–6° indicating the basal spacing (d-spacing) of the silicate layers. The d-spacing for Bt was measured at 2θ = 5.62°, with a value of 15.71 Å. The d-spacing for Bt@star was slightly shifted to a higher angle, 2θ = 5.97°, with a value of 14.77 Å. This shift in the d-spacing suggests that the presence of starch polymer constricted the interlayer galleries of bentonite. It should also be noted that the chains of the polymer are mainly located on the outer surface of the bentonite clay. Angkawijaya et al. 2020, reported similar behavior when modifying bentonite with chitosan.[22]

Furthermore, as shown in Figure 1b, the d-spacing for Bt@star@gly shifted to a lower angle of 2θ = 5.03° with a value of 17.55 Å. This increase in the d-spacing value confirms the success of the modification and the presence of glycerol in the basal space. These findings are consistent with results obtained using other molecules and macromolecules to modify bentonite, such as hexadecyltrimethylammonium bromide, cationic surfactant cetytrimethyl ammonium bromide, graphene oxide, gelatine, and poly(N-vinylpyrrolidone).[18, 23-26]

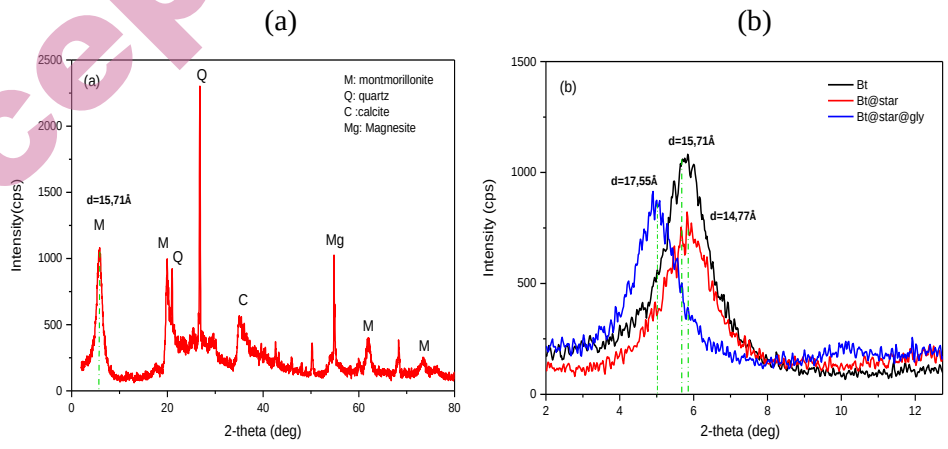

Fig. 1. XRD patterns of raw Bt (a), comparative d-basal spacing of Bt, Bt@star and Bt@star@gly (b)

The XRD results are also in agreement with FTIR analysis. Figure 2 displays the characteristic bands of corn starch, raw bentonite Bt, and the biocomposites Bt@Star and Bt@Star@glyc.

The bands (υ1 and υ2) of raw bentonite at 3625 cm^{-1} and 3701 cm^{-1} are caused by the vibrations of the OH groups of the water molecules adsorbed on the surface of the sample Bt. A broad absorption envelope (υ3) was observed in the range of 3537 cm^{-1} to 2987 cm^{-1}, which is attributed to the OH^- vibration of physically adsorbed water. Additionally, the bending mode of water was observed at 1635 cm^{-1} (υ4).[27] The IR spectrum of Bt indicates the presence of the intense band (υ5) centered at 981.51 cm^{-1}, which is related to the stretching vibration of the Si-O bonds. The 922 cm^{-1} (υ6) band reveals the presence of amorphous SiO_2.[28] Moreover, the bands at 688 cm^{-1} and 775 cm^{-1} (υ7) are attributed to the Al-O-Si-O bond and silanol group, respectively.

The FTIR spectra of Bt@Star and Bt@Star@glyc unquestionably exhibited a profile similar to that of raw bentonite. In addition, the spectra confirm the successful modification with the emergence of new bands at 2930 cm cm^{-1} (υ8) and around 1400 cm cm^{-1} (υ9). These bands are attributed to the stretching vibration of the C-H bonds and the symmetric deformation of CH_2 groups and asymmetric stretching of C-H bonds.[29] The Bt@Star spectrum and the Bt@Star@glyc spectrum are clearly distinguishable. The two bands in question are more prominent in the Bt@Star@glyc composite. This is due to the presence of similar absorption bands in the glycerol spectra.[30] This observation unequivocally confirms the fixation of glycerol in the bentonite lattice, as previously demonstrated by XRD.

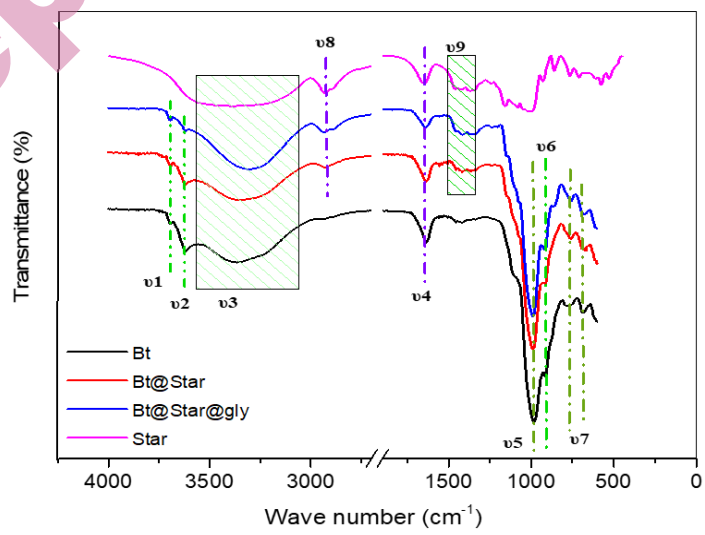

Fig. 2. FTIR spectra of the adsorbent materials

Methylene blue and red methyl dyes removal

Effect of pH

Numerous studies have shown that pH is a critical parameter in the adsorption process, as it affects both the functional groups of the adsorbent and the adsorbate. Therefore, this study investigated the removal of MB and MR dyes by native starch (Star), raw bentonite (Bt), and the composites Bt@Star and Bt@Star@glyc at three different pH values: pH 3, pH 6 and pH 9, using HCl (1 mol L^{-1}) and NaOH (1 mol L^{-1}). The results are depicted in Figure 3.

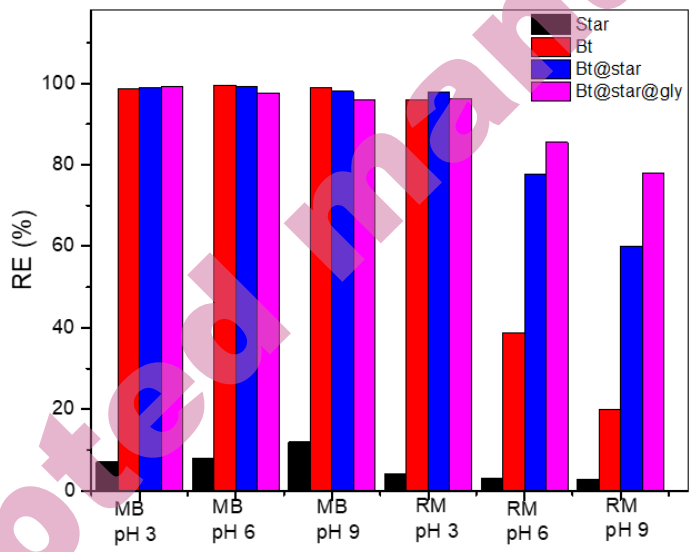

Fig. 3. MB and MR adsorption efficiency RE at different pH for Star, Bt, Bt@star and Bt@star@gly. [MB] = 100 mg/L, [MR] = 100 mg/L, V_{MB} and V_{MR} = 25 mL, m_{ads} = 25 mg, t = 60 min, T= 20°C, 400 rpm

Upon comparing the four adsorbents, the experimental data clearly show that the native corn starch has the lowest retention capacity, making it unsuitable for MB and MR retention.

The results for MB dye clearly show that Bt, Bt@star, and Bt@Star@gly have a significant and similar retention capacity (RE) at both pH 3 and pH 6 (Fig. 3). At pH 3, the RE is 98.53%, 98.99%, and 99.19% for Bt, Bt@star, and Bt@Star@gly, respectively. At pH 6, the RE is 99.46%, 99.23%, and 97.53% for Bt, Bt@star, and Bt@Star@gly, respectively.

The retention efficiency is also very significant for the MR dye at pH=6. The value increased when starch and glycerol modifiers were added to the raw bentonite. The values were 95.95% for Bt, 97.73% for Bt@star, and 96.19% for

Bt@Star@gly. The results clearly show that the addition of starch and glycerol has no negative effect on the adsorption capacity of the bentonite portion for the dyes.

The result for MR at pH=6 is undoubtedly the most important for this part. Figure 3 clearly shows a significant increase in RE (%) from 38.74% for Bt to 77.71% for Bt@Star and 85.58% for Bt@Star@gly. This result definitively confirms the crucial role of modifying Bt with starch and glycerol, which creates a structure that interacts more effectively with cationic (MB) and anionic (MR) dyes.

In contrast, it is clear that the retention efficiency of MR dye consistently decreases for all adsorbent materials as the pH varies from 3 to 6 and then to 9. This can be mainly explained by the partial deprotonation of the adsorbent surface, which gives rise to a negative charge that prevents the interaction with MR molecules that already carry a negative charge specific to their carboxylate groups.[31]

Effect of contact time

Figure 4 (a) and Figure 4 (b) show the effect of contact time on the adsorption capacity of MB and MR dyes. In these experiments, 25 mg of each adsorbent was added to 25 ml of the dyes solutions with a concentration of 100 mg L^{-1}.

As shown in Figure 4 (a), the adsorption of MB on the adsorbents Bt, Bt@star and Bt@star@gly is a fast process that can be divided into two distinct phases for the two composites. The first phase lasts for 30 minutes. During this time, the majority of the MB molecules are fixed on the surface of the adsorbents, then diffuse into the pores and the basal space of the biocomposites at a significant adsorption rate. In the second phase, the saturation of the active sites of the adsorbents resulted in a significant reduction in adsorption rate, with only a few molecules being adsorbed.

After 80 minutes of contact between the adsorbent and the adsorbate (second phase), the adsorption of MB reached a plateau, indicating that equilibrium had been reached. The presence of the plateau proves that the adsorption of MB has reached equilibrium under the considered experimental conditions and also proves that the adsorption rate is balanced by the desorption rate.

Figure 4(b) clearly shows that the adsorption of MR on the used adsorbent materials is rapid. The figure also demonstrates that the retention of MR is highly efficient, with a q_e value of more than 95 mg g^{-1} in only 5 minutes of contact time. Figure 4(b) also shows a contrasting reverse behavior to that of Figure 4(a), with minimal fluctuation in retention capacity from 5 to 60 minutes (Part 1), then a gradual desorption of the adsorbed MR molecules on Bt@star and Bt@star@Gly (Part 2).

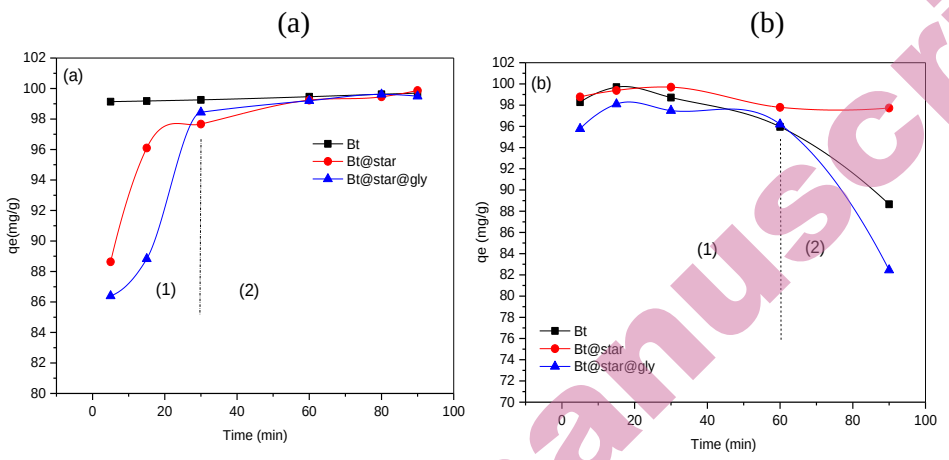

Fig. 4. Time-dependent qe (mg/g) of MB (a) and MR (b) removed by Bt, Bt@star and Bt@star@gly. [MB] = 100 mg/L, [MR] = 100 mg/L, V_{MB} and V_{MR} = 25 mL, m_{ads} = 25 mg, pH = 6, T = 20°C, 400 rpm

The experimental data were fitted with pseudo-first-order and pseudo-second-order models using Eqs. (3) and (4).

$$\text{Pseudo-first-order equation: } \log(q_e - q_t) = \log q_e - \frac{K_1}{2.303} t \quad (3)$$

$$\text{Pseudo-second-order equation: } \frac{t}{q_t} = \frac{1}{K_2 q_e^2} + \frac{1}{q_e} t \quad (4)$$

where K_1 (min^{-1}) is the pseudo-first order adsorption rate constant, K_2 (g mg^{-1} min^{-1}) is the pseudo-second order adsorption rate constant, and q_e (mg g^{-1}) is the adsorption capacity at equilibrium. These constants were determined from the slopes and intercepts of the lines obtained by plotting t/q_t versus t.

The graphical representations of this model are represented in Fig. 5, and the kinetic parameters obtained from the fitting are given in Table I. The comparison between calculated adsorption capacities $q_{e,cal}$ and experimental $q_{e,exp}$ values for each dye clearly suggests that the pseudo second order model describes the adsorption of MB and MR better. Similar results were reported by Mohammedi et al. (2020).[32-34]

In addition, the correlation coefficients (R^2) confirm that the adsorption of MB and MR on each adsorbent studied is described by the pseudo-second-order model, indicating a multistage adsorption process. The adsorption rate is therefore dependent on the number of active sites in the adsorbent material. These results are consistent with previous studies, which also found that the adsorption of methylene blue and methyl red on various materials follows the pseudo-second-order model. [35-37]

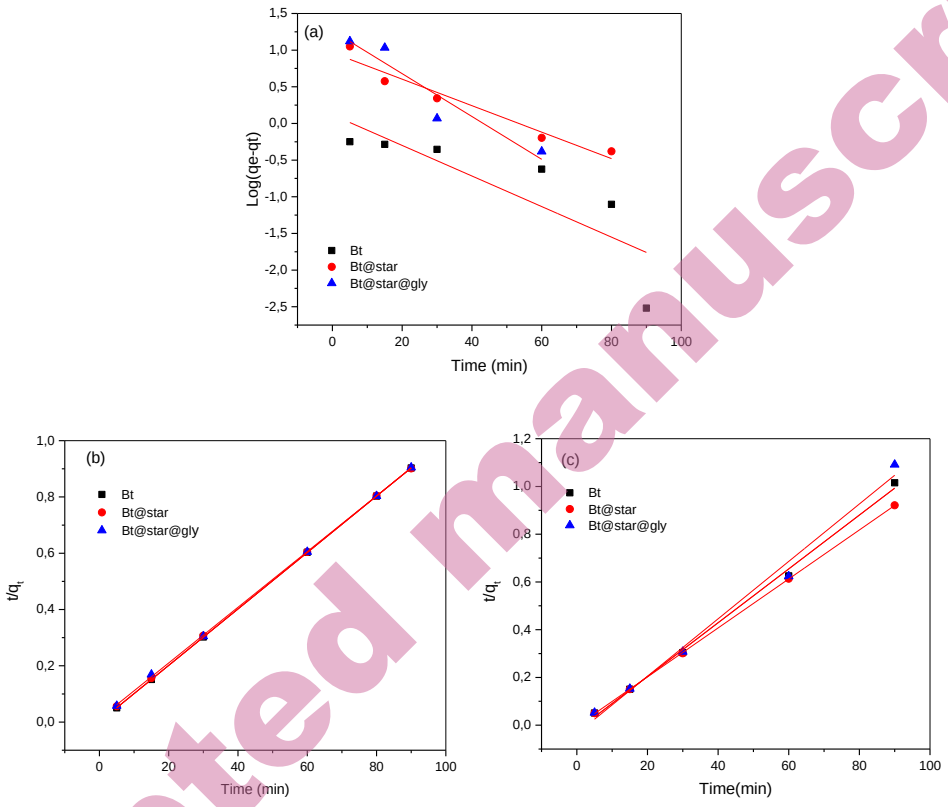

Fig. 5. Linear fit by using the pseudo-first order model of the retention of MB (a) and the linear fit by using pseudo-second order model for the retention of MB (b) and MR (c)

Table I. Characteristic parameters obtained by pseudo-first order; pseudo-second order

			1st order			2nd order		
		qe_{exp} (mg/g)	K_1 (min^{-1})	qe_{cal} (mg/g)	R^2	K_2 (mg/g.min)	qe_{cal} (mg/g)	R^2
MB	Bt	99.69	0.0479	1.31	0,703	0.1137	99.70	1
	Bt@star	99.69	0.0415	9.22	0,950	0.0134	100.50	0.999
	Bt@star@gly	99.87	0.067	18.34	0,904	$8.06\ 10^{-3}$	101.01	0,9998
MR	Bt	99.69	Not applicable			0.0113	88.65	0,9961
	Bt@star	99.61	Not applicable			0.0103	97.46	0,9999
	Bt@star@gly	98.09	Not applicable			0.0119	83.33	0,9901

Effect of MB and MR dose on the adsorption performance and isotherm study

The effect of initial dye concentration was investigated in the range of 100 to 500 mg/L^{-1}. Figure 6 (a), (b) and (c) show that the amount of dye retained by each adsorbent increases with increasing initial dye concentration. For an initial

concentration of MB equal to 500 mg L^{-1}, the adsorption capacity achieved was 203.78 mg g^{-1} (RE=40.75%), 146.21 mg g^{-1} (RE=29.24%) and 157.58 mg g^{-1} (31.51%) for Bt, Bt@star and Bt@star@gly, respectively. The MR dye q_e values are substantial, proving that the three materials are excellent adsorbents for removing both anionic and cationic dyes. The obtained adsorption capacities are equal to 309.81 mg g^{-1} (RE=61.96%), 426.38 mg g^{-1} (RE=85.27%) and 309.82 mg g^{-1} (RE=61.96%) for Bt, Bt@star and Bt@star@gly, respectively. To compare, Table II clearly shows that the composites used in this study have better adsorption capacities (q_{max}) than many other materials reported so far in the literature. [29, 38-45]

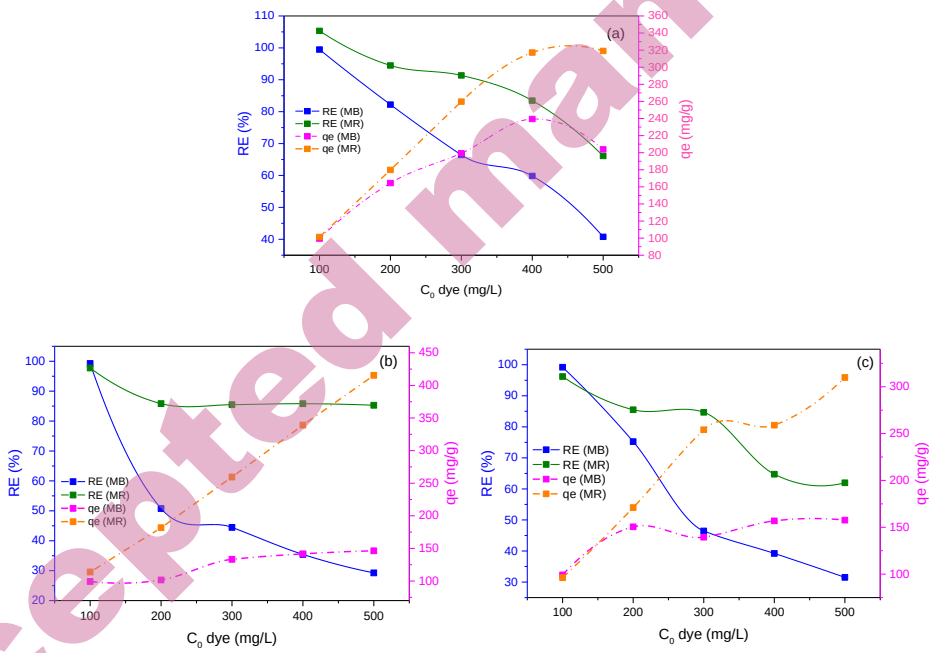

Fig. 6. MB and MR removal capacity (qe) and removal efficiency (RE) as a function of the initial dye concentration by using (a) Bt, (b) Bt@star and (c)Bt@star@gly. V_{MB} and V_{MR} = 25 mL, m_{ads} = 25 mg, pH = 6, T = 20°C, 400 rpm, t = 60 min.

Table II. Maximal adsorption capacity q_{max} (mg/g) for MB and MR removal by different materials

	Materials	q_{max} (mg/g)	Reference
MB	Hydroxyapatite@starch composite	45.51	[29]
	Calcined Hydroxyapatite	38.93	[37]
	Biogas Plant Waste	147	[38]
	Starch biocryogel	34.84	[39]
	Diatomite	66.7	[40]
	Montmorillonite modified tea waste biochar	27.89	[41]
	Bt	*203,78*	
	Bt@star	*146,21*	*This work*
	Bt@star@gly	*157.58*	
MR	Biogas Plant Waste	115	[38]
	Bark of Hopbush	36.64	[42]
	Orange peel	111.11	[43]
	Carbon clay/alginate membrane	248.14	[44]
	Anionic Surfactant	53.59	[45]
	Bt	*309.81*	
	Bt@star	*426,38*	*This work*
	Bt@star@gly	*309.82*	

In order to obtain information about the adsorption isotherms, the experimental data were fitted to the Langmuir and Freundlich adsorption models using equations (5) and (6), respectively. The curves obtained are shown in Figures 7a-d.

$$\text{Langmuir equation: } \frac{Ce}{q_e} = \frac{1}{K_1 Q_{max}} + \frac{Ce}{Q_{max}} \quad (5)$$

$$\text{Freundlich equation: } \log q_e = \log K_F + \frac{1}{n}\log C_e \quad (6)$$

where K_l is the Langmuir constant (L mg^{-1}), Q_{max} is the maximum adsorption capacity (mg g^{-1}), C_e the concentration at equilibrium (mg L^{-1}), K_F the Freundlich constant (mg g^{-1}) and n is the adsorption intensity.

Table III shows the values obtained for the constant parameters of the Langmuir and Freundlich adsorption isotherms. The correlation coefficient values clearly indicate that the adsorption of MB and MR dyes onto Bt and Bt@star@gly is better described by the Langmuir model. The applicability of the Langmuir model suggests that the adsorbent surface is homogeneous, resulting in monolayer adsorption. This unequivocally demonstrates that all the binding sites present in Bt and Bt@star@gly are energetically equivalent.

The Langmuir model also describes the adsorption of MB by the composite material Bt@Star. Nevertheless, the Freundlich isotherm model is the best fit for the adsorption of MR, indicating the existence of multilayer adsorption. This explains the important adsorption capacity of 426.38 mg g^{-1} at an initial MR concentration of 500 mg L^{-1}.

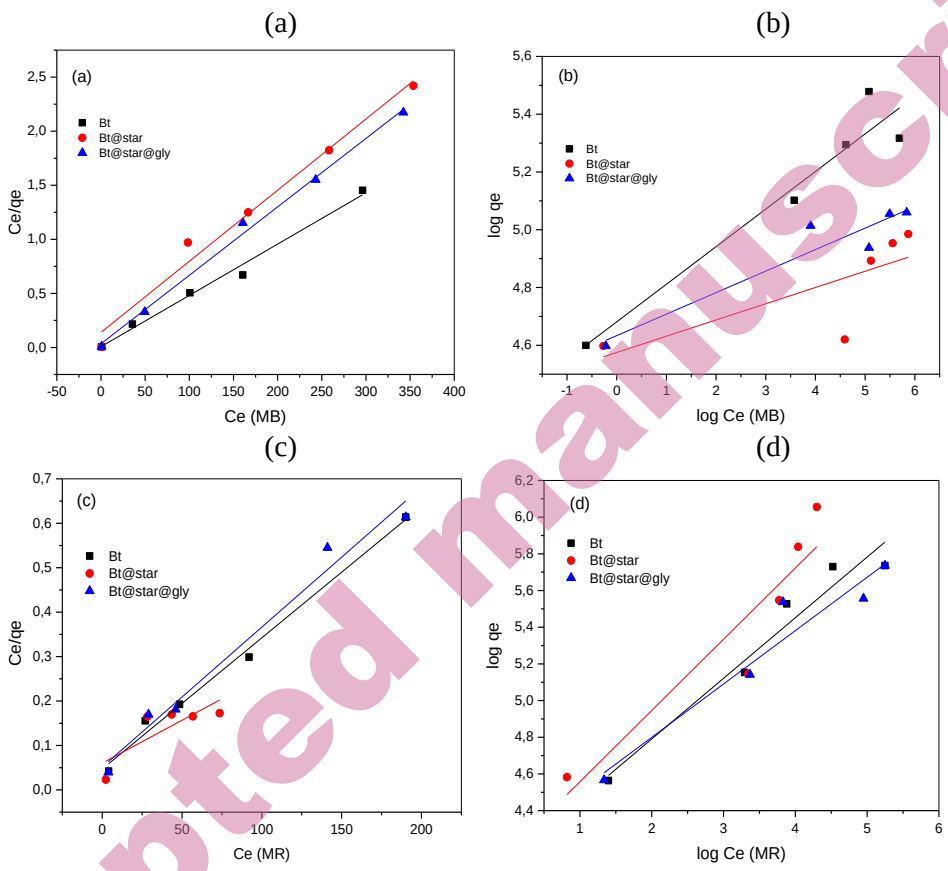

Fig. 7. Linear fits of the experimental data of MB by using Langmuir (a) and Freundlich (b) and linear fits of the experimental data of MR by using Langmuir (c) and Freundlich (d) isotherm models.

Table III. Isotherm parameters for MB and MR adsorption by Bt, Bt@star and Bt@star@gly samples according to Langmuir and Freundlich models.

		Freundlich			Langmuir		
		n	KF	R2	qmax (cal)	Kl	R2
Bt	MB	7.6863	107.8994	0.909	210.97	0.661	0.986
	MR	3.0257	62.1592	0.938	338.98	0.063	0.989
Bt@star	MB	17.7935	97.0474	0,441	151.98	0.051	0.978
	MR	2.5753	64.6831	0.827	518.13	0.032	0,543
Bt@star@gly	MB	13.4408	102.8734	0,874	157.98	0.184	0.994
	MR	3.4376	67.8771	0.913	317.46	0.061	0.973

CONCLUSION

The present investigation yielded significant results regarding the adsorption of methylene blue and methyl red using bentonite and its composites. Modification significantly improves the adsorptive capacity of bentonite, making these composites highly effective adsorbents for anionic dyes. Furthermore, the study proves that using readily available natural materials is the most effective way to minimize both starting material costs and experimental expenses. The application of adsorption on modified bentonite is undoubtedly a promising approach for the removal of pollutants from water.

И З В О Д

ПОБОЉШАНА СВОЈСТВА АДСОРПЦИЈЕ АЛЖИРСКОГ БЕНТОНИТА МОДИФИКОВАНОГ СКРОБОМ И ГЛИЦЕРОЛОМ ЗА ЗАДРЖАВАЊЕ МЕТИЛЕНСКОГ ПЛАВОГ И МЕТИЛ ЦРВЕНОГ

FATIMA ZAHRA BENHACHEM[1,2], HANANE MAHROUG[2,3], MERIEM BENDJELLOUL[4], ABDELKADER MIRAOUI[1,2], EL HADJ ELANDALOUSSI[4], KHALIL OUKEBDANE[2], RANIA HALFAOUI[5]

[1]Department of Industrial Engineering, Faculty of Technology, University of Tlemcen, Tlemcen, Algeria, [2]Laboratory of Separation and Purification Technologies, Department of Chemistry, Faculty of Sciences, University of Tlemcen, Tlemcen, Algeria, [3]Department of Hydraulic, Institute of Sciences and Technology, University center of Maghnia, Algeria. [4]Environment and Sustainable Development Laboratory, Department of Chemistry, Faculty of Sciences and Technology, University of Relizane, Algeria, and [5]Department of Chemistry, Faculty of Sciences, University of Tlemcen, Tlemcen, Algeria.

У раду је описана припрема нових композита бентонит-скроб и оцењена је њихова ефикасност као адсорбенса за уклањање боја метилен плавог (МВ) и метил црвеног (МС) из водених раствора. Адсорбенси су окарактерисани коришћењем рендгенске дифракције и FTIR спектроскопије. Студија је имала за циљ да оптимизује процес уклањања боја испитивањем утицаја pH, дозе адсорбенса, времена контакта и почетне концентрације. Кинетика сорпције МВ и МС боје је анализирана коришћењем модела псеудо првог и псеудо другог реда. Експериментални резултати показују да кинетички модел псеудо-другог реда најбоље одговара. Композитни адсорбенси су показали сорпциони капацитет за МБ у распону од 146,21 mg g^{-1} до 157,58 mg g^{-1} за бентонит-скроб (Bt@star) и бентонит-скроб-глицерол (Bt@star@gly), респективно. Капацитет сорпције за МС боју био је 426,38 mg g^{-1} за Bt@star и 309,82 mg g^{-1} за Bt@star@gly. Штавише, вредности коефицијента корелације показују да се адсорпција МБ и МР од стране Bt@star@gly најбоље описује Лангмуировим моделом. Ово недвосмислено имплицира да је површина адсорбенса хомогена, што резултира једнослојном адсорпцијом. Лангмуир модел такође тачно описује адсорпцију МВ на Bt@star. Међутим, Фројндлихов модел изотерме је најбољи за адсорпцију МР, што указује на постојање вишеслојне адсорпције. Коначно, ова студија показује да композитни адсорбенти који су овде припремљени показују одличне перформансе адсорпције и могу бити исплатива алтернатива за третман обојене отпадне воде.

(Примљено 29. фебруара; ревидирано 22. априла; прихваћено 24. новембра2024.)

REFERENCES

1. K. Nagaraja, M. Arunpandian, T. H. Oh, *J. Polym. Environ*. **32** (2024) 4538 (https://doi.org/10.1007/s10924-024-03225-5)
2. A. A. Adesibikan, S. S. Emmanuel , C. O. Olawoyin, P. Ndungu, *J. Organ. Chem*. **1010** (2024) 123087 (https://doi.org/10.1016/j.jorganchem.2024.123087)
3. S. Dutta, S. Adhikary, S. Bhattacharya, D. Roy, S. Chatterjee, A. Chakraborty, D. Banerjee, A. Ganguly, S. Nanda, P. Rajak, *J. Env. Man*. **353** (2024) 120103 (https://doi.org/10.1016/j.jenvman.2024.120103)
4. M. B. Etsuyankpa, A. U. Augustine, S. T. Musa, J. T. Mathew, H. Ismail, A. M. Salihu, A. Mamman, *J. App. Sci. Env. Manag.* **28** (2024) 5 (https://doi.org/10.4314/jasem.v28i5.28)
5. R. J. Kadhim, F. H. Al-Ani, Muayad Al-shaeli, Q. F. Alsalhy, A. Figoli, *Membranes* **10** (2020) 366 (https://doi.org/10.3390/membranes10120366)
6. I. A. Saleh, N. Zouari, & M. A. Al-Ghouti, *Env. Techn. Innov*. **19** (2020) 2352 (https://doi.org/10.1016/j.eti.2020.101026)
7. I. Mahboob, I. Shafiq, S. Shafique, P. Akhter, M. Munir, M. Saeed, M. S. Nazir, U.-e-S. Amjad, F. Jamil, N. Ahmad, Y.-K. Park, M. Hussain, *Chemosphere* **311** (2023) 137180 (https://doi.org/10.1016/j.chemosphere.2022.137180)
8. F. Z. Benhachem, M. Bendjelloul, H. Mahroug, A. Miraoui, E.H. Elandaloussi, K. Oukebdane, R. Halfaoui, *J. Dispers. Sci. Technol*. (2024) (https://doi.org/10.1080/01932691.2024.2378193)
9. L. Sablii, O. Obodovych, V. Sydorenko, *J. Serb. Chem. Soc.* (2024) (https://doi.org/10.2298/JSC231206014S)
10. A. Miraoui, L. Mitiche, F.Z. Benhachem, S. Feddane, M. Bendjelloul, E.H. Elandaloussi, M.A. Didi, *Iran. J. Chem. Chem. Eng*. **43** (2024) 3989 (https://doi.org/10.30492/ijcce.2024.2025988.6527)
11. S. Lin, Z. Song, G. Che, A. Ren, P. Li, C. Liu, J. Zhang, *Micro. Meso. Mater*. **193** (2014) 27 (https://doi.org/10.1016/j.micromeso.2014.03.004)
12. H. Gadouri, K. Harichane, M. Ghrici, *Per. Poly. Civ. Eng*. **61** (2017) 256 (https://doi.org/10.3311/PPci.9359)
13. S. Mishra, L. Cheng, A. Maiti, *J. Env. Chem. Eng*. **9** (2021) 104901 (https://doi.org/10.1016/j.jece.2020.104901)
14. R. Marouf, N. Dali, N. Boudouara, F. Ouadjenia, F. Zahaf, *Study of Adsorption Properties of Bentonite Clay* in *Montmorillonite Clay*, Ed. F. Uddin, *IntechOpen*. (2021) (https://doi.org/10.5772/intechopen.96524)
15. F. Bergaya, G. Lagaly, *Dev.Clay Sci.* **1** (2006) 1 (https://doi.org/10.1016/S1572-4352(05)01001-9)
16. R. Zhu, Q. Chen, Q. Zhou, Y. Xi, J. Zhu, H. He, *App. Clay Sci*. **123** (2016) 239 (https://doi.org/10.1016/j.clay.2015.12.024)
17. E. M. Ö. Kaya, A. S. Özcan, Ö. Gök, A. Özcan, *Adsorption* **19** (2013) 879 (https://doi.org/10.1007/s10450-013-9542-3)
18. Z. Baouch, K.I. Benabadji, B. Bouras, *Phys. Chem. Res*. **8** (2020) 767 (https://doi.org/10.22036/pcr.2020.234691.1787)
19. L. Wang, A. Wang, *J. Haz. Mat.* **160** (2008) 173 (https://doi.org/10.1016/j.jhazmat.2008.02.104)
20. Ö. Açışlı, S. Karaca, A. Gürses, *App. Clay Sci.* **142** (2017) 90 (https://doi.org/10.1016/j.clay.2016.12.009)

21. S. Yang, M. Gao, Z. Luo, *Chem. Eng. J.* **256** (2014) 39 (https://doi.org/10.1016/j.cej.2014.07.004)
22. A. E. Angkawijaya, S. P. Santoso, V. Bundjaja, F. E. Soetaredjo, C. Gunarto, A. Ayucitra, Y. Ju, A.W. Go, S. Ismadji, *J. Hazard. Mat.* **399** (2020) 123130 (https://doi.org/10.1016/j.jhazmat.2020.123130)
23. P. Huang, A. Kazlauciunas, R. Menzel, L. Lin, *ACS Appl. Mater. Inter.* **31** (2017) 26383 (https://doi.org/10.1021/acsami.7b08406)
24. Z. Taibi, K. Bentaleb, Z. Bouberka, C. Pierlot, M. Vandewalle, C. Volkringer, P. Supiot, U. Maschke, *Crystals* **13** (2023) 211 (https://doi.org/10.3390/cryst13020211)
25. S. Merad Boudia, K. I. Benabadji, B. Bouras, *Phys. Chem. Res.* **33** (2022) 143 (https://doi.org/10.22036/pcr.2021.290926.1925)
26. D. Heddi, A. Benkhaled, A. Boussaid, E. Chekchou Braham, *Phys. Chem. Res.* **7** (2019) 731 (https://doi.org/10.22036/pcr.2019.179510.1625)
27. K. Atkovska, B. Bliznakovska, G. Ruseska, S. Bogoevski, B. Boskovski, A. Grozdanov, *J. Chem. Technol. Metall.* **51** (2016) 215
28. B. Makhoukhi, M. Djab, M. A. Didi, *J. Environ. Chem. Eng.* **3** (2015) 1384 (https://doi.org/10.1016/j.jece.2014.12.012)
29. H. Mahroug, S. Belkaid, *Phys. Chem. Res.* **12** (2023) 73 (https://doi.org/10.22036/pcr.2023.374016.2244)
30. M. R. Nanda, Z. Yuan, W. Qin, M. A. Poirier, X. Chunbao, *Austin J. Chem. Eng.* **1** (2014) 1004 (https://austinpublishinggroup.com/chemical-engineering/fulltext/ace-v1-id1004.php)
31. S. Rangabhashiyam, N. Anu, N. Selvaraju, *J. Envir. Chem. Engin.* **1 (**2013**)** 629 **(**https://doi.org/10.1016/j.jece.2013.07.014)
32. S. Z. Mohammadi, N. Mofidinasab, M.A. Karimi, A. Beheshti, *Int. J. Environ. Sci. Technol.* **17** (2020) 4815 (https://doi.org/10.1007/s13762-020-02767-0)
33. S. Z. Mohammadi, Z. Safari, N. Madady, *Appl. Surf. Sci.* **514** (2020) 145873 (https://doi.org/10.1016/j.apsusc.2020.145873)
34. S. Z. Mohammadi, N. Mofidinasab, M. A. Karimi, F. Mosazadeh, *Water. Sci. Technol.* **82** (2020) 829 (https://doi.org/10.2166/wst.2020.375)
35. M. El-Habacha, A. Dabagh, S. Lagdali, Y. Miyah, G. Mahmoudy, F. Sinan, M. Chiban, S. Laich, M. Zerbet, *Environ. Sci. Pollut. Res.* (2023) (https://doi.org/10.1007/s11356-023-27413-3)
36. Y. A. B. Neolaka, Y. Lawa, J. Naat, A. C. Lalang, B. A. Widyaningrum, G. F. Ngasu, K. A. Niga, H. Darmokoesoemo, M. Iqbal, H. S. Kusuma, *Results. Eng.* **17** (2023) 100824 (https://doi.org/10.1016/j.rineng.2022.100824)
37. M. Aaddouz, K. Azzaoui, N. Akartasse, E. Mejdoubi, B. Hammouti, M. Taleb, R. Sabbahi, S. F. Alshahateet, *J. Mol. Struct.* **1288** (2023) 135807 (https://doi.org/10.1016/j.molstruc.2023.135807)
38. R. Wolski, A. Bazan-Wozniak, R. Pietrzak, *Molecules* **28** (2023) 6712 (https://doi.org/10.3390/molecules28186712)
39. T. Taweekarn, W. Wongniramaikul, C. Boonkanon, C. Phanrit, W. Sriprom, W. Limsakul, W. Towanlong, C. Phawachalotorn, A. Choodum, *Polymers* **14** (2022) 5543 (https://doi.org/10.3390/polym14245543)
40. N. A. Fathy, S. M. Mousa, R.M. Aboelenin, M.A. Sherief, A. S. Abdelmoaty, *Arab. J. Geosci.* **15** (2022) 1664 (https://doi.org/10.1007/s12517-022-10891-z)
41. R. Liu, Y. C. Li, Z. Zhao, D. Liu, J. Ren, Y. Luo, *Front. Environ. Sci.* **11** (2023) 1137284 (https://doi.org/10.3389/fenvs.2023.1137284)

42. S. Gul, M. Kanwal, R. A. Qazi, H. Gul, R. Khattak, M. S. Khan, F. Khitab, A. E. Krauklis, *Water* **14** (2022) 2831 (https://doi.org/10.3390/w14182831)
43. S. Deshmukh, N. S. Topare, S. Raut-Jadhav, P. V. Thorat, S. A. Bokil, A. Khan, *Aqua Water. Infrastruct. Ecosyst. Soc*. **71** (2022) 1351 (https://doi.org/10.2166/aqua.2022.119)
44. N. Ullah, Z. Ali, A. Sada Khan, B. Adalat, A. Nasrullah, S. Bahadar Khan, *RSC. Adv*. **14** (2024) 211 (https://doi.org/10.1039/D3RA07554K)
45. Y. N. Teixeira, J. M. C. Menezes, R. N. P. Teixeira, F. J. Paula Filho, T. M. B. F. Oliveira, *Textiles* **3** (2023) 52 (https://doi.org/10.3390/textiles301000).